

7C BED SEDIMENT: CHARACTERISATION, ENTRAINMENT THRESHOLDS AND TRANSPORT RATES

7C.1 INTRODUCTION

The objective of this assessment is to investigate the potential impact of the proposed flood relief scheme, comprising a culvert 'Flow Control' structure and weir diversion of high flows, on bedload entrainment and transport in the River Deel, and the implications for morphological adjustment.

In the majority of gravel-bed rivers the main source of bedload material is the channel bed. Where sediment is readily available for transport, bedload transport is limited by the transporting capacity of the flow, although bed armouring (the build-up of a coarse surface layer) can restrict supply (Knighton, 1998). In most fluvial systems bedload material does not constitute the highest proportion of the total sediment load (compared to solute and suspended load), but it does play an important role in channel morphodynamics. Therefore, changes in channel hydraulics or sediment delivery that alter bedload transport rates can lead to morphological adjustment and changes in habitat availability, although these effects can be subtle and relatively localised, such as the bed sediment coarsening observed immediately downstream of low-head dams (Casserly et al., 2020). Because of the complex and highly variable nature of bed material movement, determining thresholds for bedload entrainment and accurate bedload transport rates is challenging (the accuracy of quantitative estimates is highly variable). More reliable bedload transport data can be obtained from direct monitoring, but where this is not feasible, the application of predictive models using established empirical relations has been used as an alternative. These models incorporate particle size statistics from the current channel bed, based on the assumption that these sediments are representative of equilibrium or reference bedload transport conditions in the system. Where relative changes in entrainment thresholds and transport rates are sufficient to provide an indication of the geomorphic impact of disturbance, this approach provides a practical and viable alternative to direct monitoring.

In this report we apply two complimentary approaches based upon estimates of bed shear stress using established empirical relations for gravel-cobble streams (details are provided below). The work has been carried out employing the HEC-RAS 1D models for the Deel (before and after installation of the flood relief scheme) and baseline bed sediment data for specific 'reaches' along the channel.

7C.2 ASSESSMENT METHODOLOGY

7C.2.1 Reach Selection and Bedload Characterization

Four reaches were selected along a section of the River Deel based upon the channel long-profile, the proposed location of the culvert flow control structure and Jack Garrett Bridge in the town of Crossmolina. This sub-division of the channel is somewhat arbitrary, but nevertheless facilitates an assessment of the River

Deel upstream and downstream of the Flow Control structure, together with some consideration of longitudinal trends in the vicinity of the town of Crossmolina.

Reach 1 comprises a c. 500 m stretch of the channel immediately upstream of the proposed Flow Control structure and has a mean bed slope of 0.00138 m/m. Reach 2 has a length of 770 m from the culvert to Jack Garrett bridge. For c. 500 m of this reach the channel bed slope is similar to Reach 1 ($s = 0.00168$ m/m), but thereafter the bed rises towards Jack Garrett bridge giving a marginally negative bed slope for the entire reach of -0.0009 m/m. Reaches 3 and 4 subdivide the next kilometre of channel, and have bed slopes of c. 0.00366 m/m and 0.0080 m/m, respectively. Although flow geometries do vary within each reach, broadly representative cross-sections (derived from the HEC-RAS model) are shown in Figure 1.

During a field visit in August 2019 when portions of the channel bed were dry, the bed material along this stretch of the Deel was observed to be predominantly homogenous and gravel-dominated, with no obvious accumulations of fines or distinctive geomorphic units. Bed sediment sampling was therefore conducted in a zig-zag pattern along each reach (Butte and Abt, 2001) using traditional Wolman (1954) pebble counts, with sediment calibre measured along the b-axis for each clast. Tabulated particle size data including sample counts are given in Appendix 1.

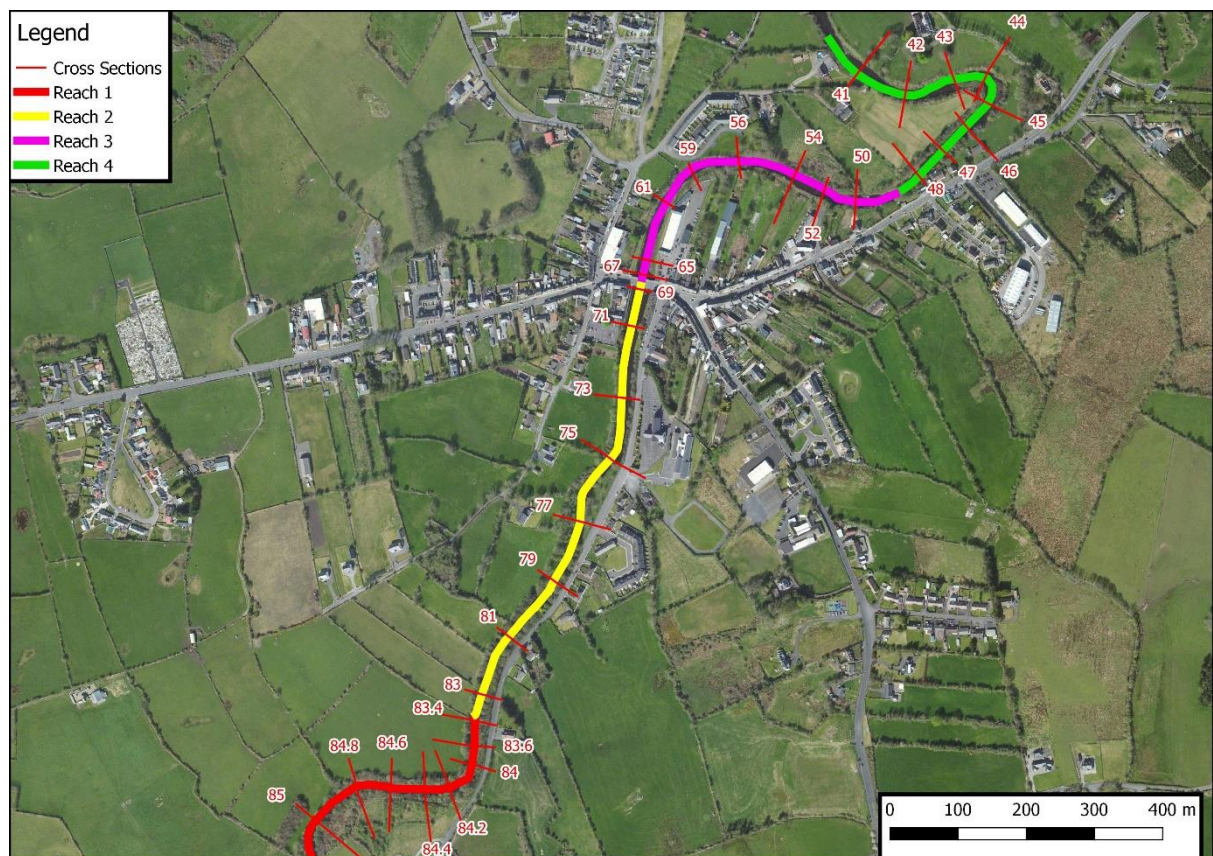


Figure 1. Location of reaches and cross-sections

7C.2.2 Estimates for bed shear stress

Mean and ‘maximum’ channel shear stress (N/m^2) were estimated for Reaches 1 to 4, for a range of pre- and post-work discharges (5 - 180 m^3/s), capturing return periods up to the nominal ‘100-year flood’, using the HEC-RAS 1D model. Mean channel shear is a depth-averaged value reported by HEC-RAS that can underestimate shear stress at the bed so a ‘maximum’ channel shear stress (albeit still potentially underestimating peak bed shear) was also calculated by replacing the hydraulic radius parameter with maximum channel depth (computed for each cross-section using HEC-RAS 1D). Critical shear stress (τ_{ci}) for the particle size of interest (D_i) was calculated using the empirical relation used by Parker et al. (2011):

$$\tau_{ci} = (0.19 \cdot S^{0.28}) \cdot (\rho_s - \rho_w) \cdot g \cdot D_i \quad (1)$$

where g is the acceleration due to gravity [9.81 m/s^2], ρ_w is the density of water [1000 kg/m^3], ρ_s is the density of bed sediment [2711 kg/m^3 for limestone - the predominant bed sediment in the Deel], S is water surface slope for a nominal high flow approximately equivalent to reach-average bankfull discharge (derived from HEC-RAS) and D_i is the bed sediment calibre of interest [D_{16} to D_{84}].

7C.2.3 Estimating bedload transport rates using BAGS

Bedload transport rates (kg/min) have been estimated for Reaches 1-4 using the surface-based relation of Wilcock and Crowe (2003). This empirically-based model, which accounts for the non-linear effect of the channel’s sand content on transport rates, was selected based on its performance against eight others on replicating the transport rates derived from a field study (Vázquez-Tarrío and Menéndez-Duarte, 2014, 2015). Calculations were made using the United States Department of Agriculture’s BAGS (Bedload Assessment for Gravel-bed Streams) software programme (Pitlick et al., 2009; Wilcock et al., 2009), which models transport as a ratio of available shear stress to the threshold shear stress. Transport potential for each reach was calculated based on field measurements of cross-sectional geometry, particle size distribution, flow data, Manning’s roughness coefficients and modelled reach-average water surface slope. However, interpretation of absolute values should be undertaken with caution as bedload transport outputs have been shown to differ by several orders of magnitude, partly due to uncertainties and potential errors in model input variables.

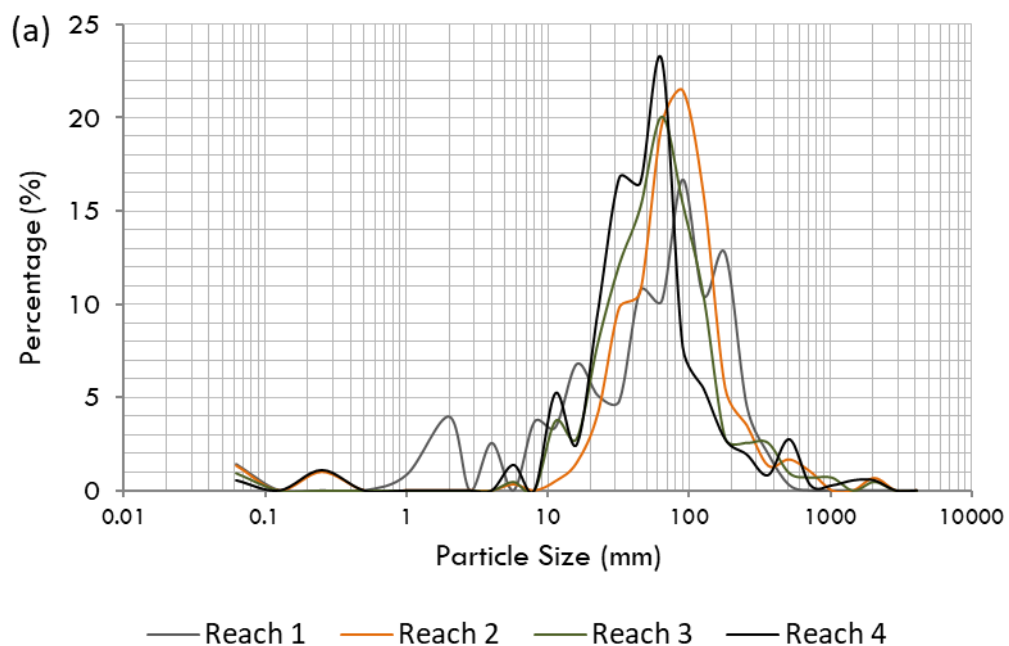
7C.3 RESULTS

7C.3.1 Bed material particle size

Percentage and cumulative percentage particle size distributions are shown in Figures 2a and 2b, respectively. Summary data for specific particle size fractions ranging from the 16th percentile (D_{16}) to the 95th percentile (D_{95}) are shown in Table 1 (tabulated results are given in Appendix 1). Note that values for upper and lower percentiles have lower precision (Butte and Abt, 2001). All four reaches are gravel-cobble dominated, with the coarsest bed material found in Reach 2 where the bed gradient is lowest. Except for

the D_{25} fraction, the least coarse sediment was recorded in Reach 4 below Crossmolina, indicating modest downstream fining across the c. 2 km stretch.

A Two-sample Kolmogorov-Smirnov test was used to determine if differences in the particle size distributions were statistically significant between reaches, with H_0 stating that there was no significance. Results for all research pairs were observed to be highly significant (meaning the H_0 could be rejected), with the highest D statistic for adjacent reaches reported for Reach 1 v Reach 2 ($R1 \text{ v } R2, D = .189, p < 0.01$; $R2 \text{ v } R3, D = .144, p < .01$; $R3 \text{ v } R4, D = .135, p < .01$; $R1 \text{ v } R3, D = .147, p < .01$, $R1 \text{ v } R4, D = .235, p < .01$; $R2 \text{ v } R4, D = .279, p < .01$).



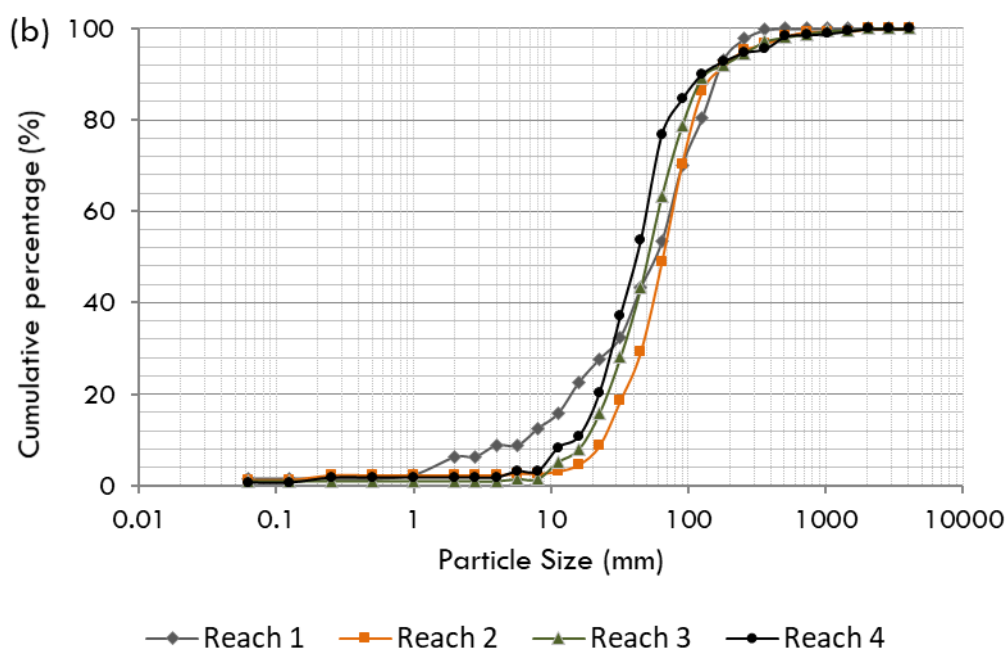


Figure 2. Particle size (a) and cumulative particle size (b) distributions for the Deel reaches (1-4)

Table 1 Particle size data (mm) for Wolman pebble counts on the River Deel in 2019

Reach	D ₁₆	D ₃₅	D ₅₀	D ₆₅	D ₈₄	D ₉₅
1	16 mm	36	49	65	89	169
2	29	51	65	83	121	249
3	23	38	51	67	108	271
4	20	31	42	54	88	286

7C.3.2 Estimates for channel shear vs. critical shear stress

Pre- and post-work estimates for depth-averaged channel shear and ‘maximum’ shear are shown in Figure 3, together with the critical shear stress thresholds for specific particle size fractions calculated using Eq. 1 (after Parker et al., 2011). Both mean channel shear and ‘maximum’ shear show consistent patterns and changes as discharge increases. In the pre-works channel upstream of the culvert, shear stress values are generally higher than the corresponding post-works channel under most flows, although for most cross-sections shear stress plateaus between 60 m³/s and 90 m³/s. Following installation of the culvert flow control structure and diversion channel both the channel and ‘maximum’ shear stress values peak at 50 or 60 m³/s in cross-sections 83.4 to 84.2 of Reach 1, with these peak shear stress values c. 30% lower than the equivalent flow in the current channel. In contrast, cross-sections 84.4 through to 85 show a marked increase in shear stress from 80 m³/s, with shear stress values exceeding those in the pre-works channel above 130 m³/s (≈10-yr event). In terms of the critical shear stress values, most cross-sections achieve a maximum shear stress above the estimated τ_{ci} for the D₈₄ fraction in the pre-works channel, while in the post-works channel aside from cross-section no. 84, none of the stations below the diversion channel records a maximum shear stress >26.7 N/m² required to mobilise the current D₆₅ particle size fraction. Downstream of the culvert, the magnitude of shear stress change with increasing discharge are quite variable within each reach, particularly

Reach 3 that displays the highest values recorded in selected cross-sections. Not all of the cross-sections achieve maximum shear stress values above the estimated τ_{ci} for the D_{84} fraction.

7C.3.3 Estimated bedload transport rates using BAGS

Estimated fractional transport rates [kg/min] for nominal low ($20 \text{ m}^3/\text{s}$), intermediate ($59 \text{ m}^3/\text{s}$) and high flows ($130 \text{ m}^3/\text{s}$), are shown in Figure 4. The patterns are consistent across all flows with higher transport rates predicted for Reach 3. These are approximately an order of magnitude higher than estimated bedload transport rates for the other reaches in the current channel. Transport rates in Reach 2 (i.e. across all particle size fractions) are about half those reported for the current Reach 1 channel. Installation of the culvert flow control structure leads to drop in reach-averaged transport rates for Reach 1 across all particle size fractions by approximately 50%, with average transport rates of $4.93 \times 10^{-5} \text{ kg/min}$ and $9.90 \times 10^{-6} \text{ kg/min}$ reported for the pre- and post-works channel, respectively.

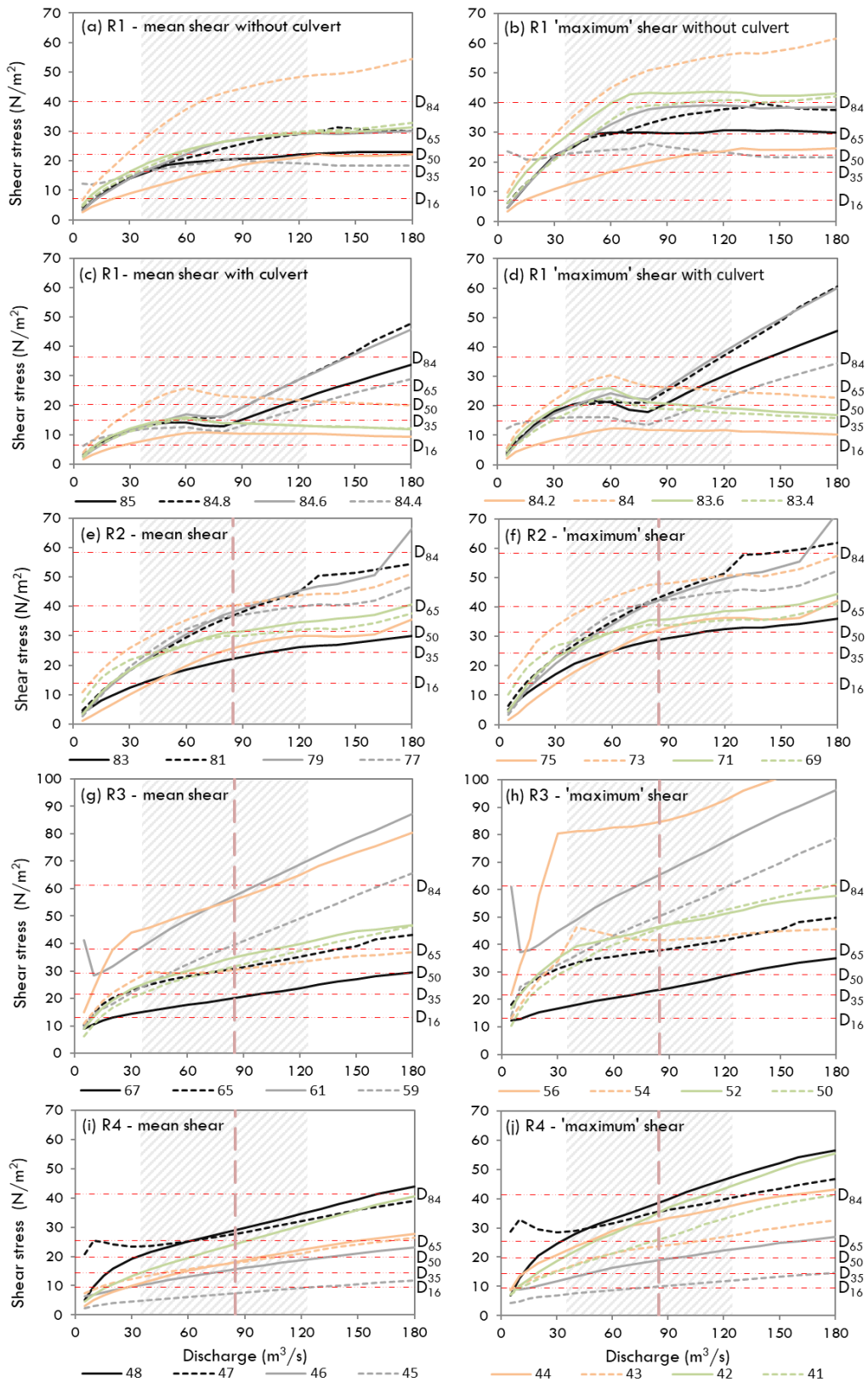


Figure 3. Depth-averaged and maximum shear for selected cross-sections in Reaches 1 to 4 (i.e. from station 85 to station 40). Horizontal dashed lines indicate the estimated critical shear stress for specific particle size fractions (D_{16} to D_{84}). The vertical dashed line marks the maximum design flow downstream of the culvert flow control structure ($85 \text{ m}^3/\text{s}$) and the hashed-shaded area represents a range of flood flows from the 1% flood (c. $35 \text{ m}^3/\text{s}$) to the 10-year flood (c. $125 \text{ m}^3/\text{s}$).

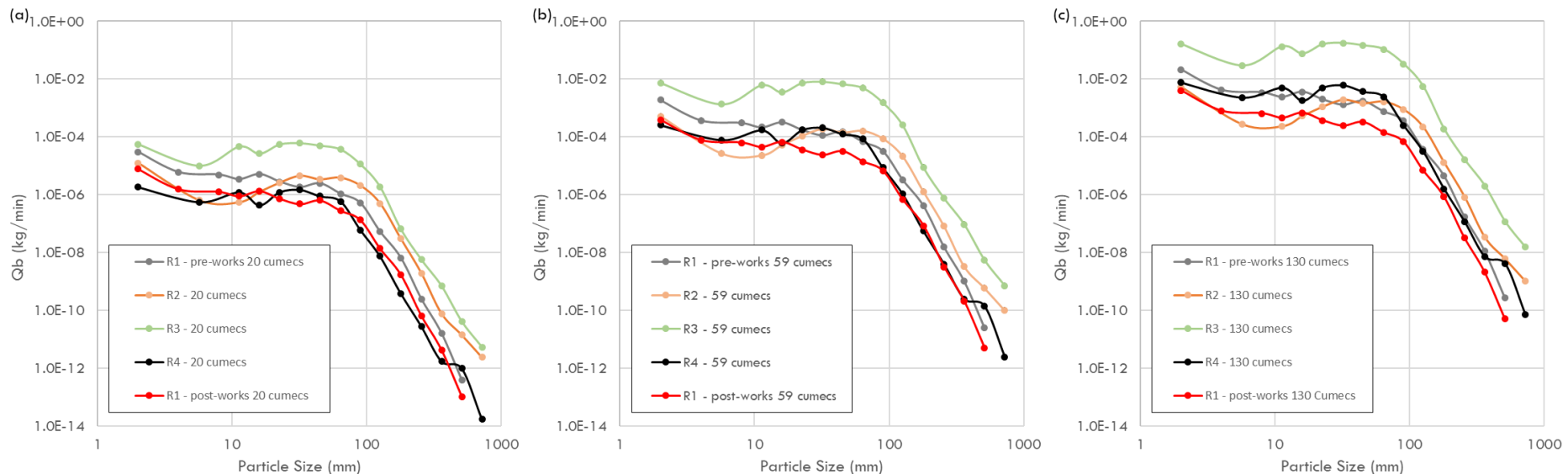


Figure 4. Reach-averaged fractional bedload transport rates [kg/min] for selected flows estimated using the surface-based relation of Wilcock and Crowe (2003). Calculations were made using the United States Department of Agriculture's BAGS (Bedload Assessment for Gravel-bed Streams) software programme (Pitlick et al., 2009)

7C.4 DISCUSSION

7C.4.1 Bedload state and transport rates in the current channel

Statistically significant differences in particle size distributions between Reaches should be interpreted with some caution because of the sensitivity of the Two-sample Kolmogorov-Smirnov test. However, the relatively coarse sediment in Reach 2 does correspond to a reduction in the bed gradient along the river and may be indicative of more limited transport and corresponding aggradation along this section of the river (possibly because of the influence of Jack Garrett bridge and the town). This hypothesis is supported by the estimated 50% reduction in reach-averaged transport rates predicted by BAGS (see Figure 4), but again given the potential imprecision of these calculations, these observations are not conclusive. Bed shear stress is variable along the Deel and within the reaches adopted in this study. The highest channel shear stress values occur in Reach 3 which corresponds to the highest bedload transport rates reported by BAGS. Cross-sectional geometries of the channel show a more incised channel along parts of this reach which may be a response to the reduction in bedload transport rates upstream, particularly the movement of the coarser bedload fraction. Differences in channel slope and flow geometries along the current channel are indicative of channel adjustment in response to existing human impact and intervention. It is not clear if the system has reached dynamic equilibrium so this adjustment may be ongoing.

7C.4.2 Impact of the flood relief scheme

Critical shear stress and the estimated fractional transport rates reveal an impact on bedload mobility following the installation of the culvert flow control structure and diversion channel in Reach 1. Although absolute thresholds for entrainment are estimated, the trends suggest that these effects will reduce total bedload transport rates and the mobilisation of the coarser bedload fraction in the reaches between the channel and culvert. Upstream of the proposed diversion channel, the increased channel efficiency resulting from the change in hydraulics is giving higher shear stress values under very high flows, which contrasts with the predicted changes immediately downstream. The HEC-RAS 1D model does not capture post-works geomorphic adjustment, but consideration should nevertheless be given to the hydromorphological response of the system to the anticipated reduction in transport rates in Reach 1 and therefore sediment input to Reach 2, in the context of the reduction in peak flows downstream.

Determining an accurate trajectory for post-works channel adjustments will require monitoring, but in principle a reduction in transport capacity in the lower cross-sections of Reach 1 (83.4 to 84.2), under the same sediment regime is likely to see aggradation along this stretch of the channel. This is supported by the outputs of the reach-averaged bedload transport rates from BAGS. These adjustments may also be accompanied by local bed sediment coarsening. Because the higher shear stress values upstream (stations 84.4 to 85) only occur under rare, extreme events, the implications for the predicted changes in this stretch of the channel are likely to be less significant. The morphological adjustments in Reach 2 and further downstream will be a function of the relative impacts of reduced sediment delivery below the culvert and the reduction in peak flows. Given that entrainment thresholds (based upon critical shear stress) are achieved

for all but the largest clasts under the new design flow, a reduction in sediment input is likely to see elevated movement of the existing bed material (leading to bed reorganization and possibly localised incision downstream of the flow control structure). Morphological adjustments in all reaches can take time to propagate through the system ($>10^1$ years), with the reaches downstream of the culvert possibly experiencing a minor sediment deficit during this period in the absence of any mitigation measures (see below). The new 'equilibrium' condition will depend on channel adjustment and reorganization of the sediment delivery upstream of the culvert and trajectories of change downstream of the structure. It is anticipated that the potential effects described above will be consistent with intra-reach variability in bed shear recorded by the 1D HEC-RAS model elsewhere within the existing channel. It is worth noting that future channel adjustment will occur in the context of Climate Change that may also alter catchment-scale hydrological and sediment regimes.

7C.5 RECOMMENDATIONS

7C.5.1 Monitoring

Monitoring of any morphological adjustment and bed sediment characteristics is recommended in the vicinity of the new structures. This will ensure that any changes are recorded and if necessary, measures can be put in place to ameliorate any identified effects.

Regular field observations should be carried out following high flow periods (immediately upstream and downstream of the culvert) to assess whether any changes in bedload transport are reflected in channel adjustment. The frequency of this monitoring will depend on the hydrodynamic conditions, but we recommend this should be carried at least once a year to ensure that any potential effects are identified and action taken if required. As part of this monitoring programme it is recommended that repeated photographs and cross-section surveys (if required) are undertaken at strategic cross-sections. Repeat cross-section profiles will assist in quantifying changes to flow and channel geometry and assist in the assessment of impacts on sediment delivery below the culvert. Cross-section selection should be guided by field observations and the modelled output in Figure 3 (it would be prudent to include those cross-sections where shear stress values are most likely to be affected).

In the case that aggradation upstream of the flow control structure requires removal, particularly if this is combined with any evidence of changes to the channel downstream in Reach 2, consideration should be given to the transfer of gravels across the culvert. The timing and volume of transfer should be guided by observed changes, with downstream replenishment consistent with the transporting capacity of the channel. Intervention strategies, however, should be cognisant of natural bed reorganization and morphological adjustment which can take many years to occur in gravel-bed channels and could be the result of ongoing (both natural and anthropogenic) processes that are unrelated to the flow control structure or the diversion channel. Baseline data (e.g. local knowledge of the Deel) would be useful in assessing whether observed bed changes are related to natural sediment conveyance or a function of imposed changes in channel hydraulics. Removal of

sediment from above the culvert may require a more immediate action, however, if aggradation in this zone compromises the design objectives of the flood relief scheme.

In final conclusion, any potential effect of the Crossmolina Flood Relief Scheme (including the flow control structure and diversion channel) on the hydromorphology of the River Deel, whilst evident in the modelling undertaken, is consistent with intra-reach variability in bed shear modelled elsewhere within the existing channel. Post works monitoring frequency will depend on the hydrodynamic conditions to ensure that any potential effects are identified and ameliorated. Action taken, if required, should be informed by best practice.

7C.6 REFERENCES

- Bunte, K., Abt, S.R. 2001. *Sampling surface and subsurface particle-size distributions in wadable gravel- and cobble-bed streams for analyses in sediment transport, hydraulics, and streambed monitoring*, Gen. Tech. Rep. RMRS-GTR-74, USDA Forest Service, Rocky Mountain Research Station, Fort Collins, CO.
- Casserly, C.M., Turner, J.N., O'Sullivan, J.J., Bruen, M., Bullock, C., Atkinson, S. & Kelly-Quinn, M. 2020. Impact of low-head dams on bedload transport rates in coarse-bedded streams", *Science of The Total Environment*. In press. <https://doi.org/10.1016/j.scitotenv.2020.136908>.
- Knighton, D. A. 1998. *Fluvial Forms and Processes: A New Perspective*, Arnold, London.
- Parker, C., Clifford, N.J., Thorne, C.R. 2011. Understanding the influence of slope on the threshold of coarse grain motion: Revisiting critical stream power. *Geomorphology* **126**, 51–65.
- Pitlick, J., Cui, Y., Wilcock, P. 2009. *Manual for Computing Bed Load Transport Using BAGS*. USDA, Forest Service, Rocky Mountain Research Station, Colorado (USA).
- Vázquez-Tarrío, D., Menéndez-Duarte, R. 2014. Bedload transport rates for coarse-bed streams in an Atlantic region (Narcea River, NW Iberian Peninsula). *Geomorphology* **217**, 1–14.
- Vázquez-Tarrío, D., Menéndez-Duarte, R. 2015. Assessment of bedload equations using data obtained with tracers in two coarse-bed mountain streams (Narcea River basin, NW Spain). *Geomorphology* **238**, 78-93.
- Wilcock, P.R., Crowe, J.C. 2003. Surface-based transport model for mixed-size sediment. *Journal of Hydraulic Engineering* **129**(2), 120–128.
- Wilcock, P., Pitlick, J., Cui, Y. 2009. *Sediment Transport Primer: Estimating Bed-Material Transport in Gravel Bed Rivers*. USDA, Forest Service, Rocky Mountain Research Station, Colorado, USA.
- Wolman, M.G. 1954. A method of sampling coarse river-bed material. *Transactions American Geophysical Union* **35**(6), 951-956.

Appendix 1 – Data Tables

Table A1 – Reach-specific article size data for the River Deel, based on Wolman (1954) pebble counts conducted in August 2019

RIVER DEEL PEBBLE COUNT DATA - August 2019													
B-axis diameter (mm)*	Descriptor	Reach 1 count	% Freq.	Cum. % Freq.	Reach 2 count	% Freq.	Cum. % Freq.	Reach 3 count	% Freq.	Cum. % Freq.	Reach 4 count	% Freq.	Cum. % Freq.
<.062	Silt/Clay	5	1.4%	1.4%	8	1.3%	1.3%	4	0.9%	0.9%	2	0.6%	0.6%
.062 - .125	Very Fine	0	0.0%	1.4%	0	0.0%	1.3%	0	0.0%	0.9%	0	0.0%	0.6%
.125 - .25	Fine	0	0.0%	1.4%	6	1.0%	2.3%	0	0.0%	0.9%	4	1.1%	1.7%
.25 - .50	Medium	0	0.0%	1.4%	0	0.0%	2.3%	0	0.0%	0.9%	0	0.0%	1.7%
.50 - 1.0	Coarse	3	0.8%	2.3%	0	0.0%	2.3%	0	0.0%	0.9%	0	0.0%	1.7%
1.0 - 2	Very Course	14	4.0%	6.2%	0	0.0%	2.3%	0	0.0%	0.9%	0	0.0%	1.7%
2 - 2.8	Very Fine	0	0.0%	6.2%	0	0.0%	2.3%	0	0.0%	0.9%	0	0.0%	1.7%
2.8-4.0	Very Fine	9	2.5%	8.8%	0	0.0%	2.3%	0	0.0%	0.9%	0	0.0%	1.7%
4 - 5.7	Fine	0	0.0%	8.8%	2	0.3%	2.7%	2	0.5%	1.4%	5	1.4%	3.0%
5.7 - 8	Fine	13	3.7%	12.4%	0	0.0%	2.7%	0	0.0%	1.4%	0	0.0%	3.0%
8 - 11.3	Medium	12	3.4%	15.8%	3	0.5%	3.2%	16	3.7%	5.1%	19	5.2%	8.3%
11.3 - 16	Medium	24	6.8%	22.6%	9	1.5%	4.7%	12	2.8%	7.9%	9	2.5%	10.7%
16 - 22.6	Coarse	18	5.1%	27.7%	25	4.2%	8.8%	34	7.9%	15.9%	35	9.6%	20.4%
22.6 - 32	Coarse	17	4.8%	32.5%	59	9.8%	18.6%	52	12.1%	28.0%	61	16.8%	37.2%
32 - 45.0	Very Course	38	10.7%	43.2%	64	10.6%	29.3%	65	15.2%	43.2%	60	16.5%	53.7%
45.0 - 64	Very Course	36	10.2%	53.4%	118	19.6%	48.9%	86	20.1%	63.3%	84	23.1%	76.9%
64 - 90.0	Small	59	16.7%	70.1%	129	21.5%	70.4%	66	15.4%	78.7%	28	7.7%	84.6%
90.0 - 128	Small	37	10.5%	80.5%	96	16.0%	86.4%	45	10.5%	89.3%	20	5.5%	90.1%
128 - 180	Large	45	12.7%	93.2%	33	5.5%	91.8%	12	2.8%	92.1%	10	2.8%	92.8%
180 - 256	Large	16	4.5%	97.7%	21	3.5%	95.3%	11	2.6%	94.6%	7	1.9%	94.8%
256 - 362	Small	7	2.0%	99.7%	8	1.3%	96.7%	11	2.6%	97.2%	3	0.8%	95.6%
362 - 512	Small	1	0.3%	100.0%	10	1.7%	98.3%	4	0.9%	98.1%	10	2.8%	98.3%
512 - 724	Medium	0	0.0%	100.0%	6	1.0%	99.3%	3	0.7%	98.8%	1	0.3%	98.6%
724 - 1024	Medium	0	0.0%	100.0%	0	0.0%	99.3%	3	0.7%	99.5%	1	0.3%	98.9%
1024 - 1450	Large	0	0.0%	100.0%	0	0.0%	99.3%	0	0.0%	99.5%	2	0.6%	99.4%
1450 - 2048	Large	0	0.0%	100.0%	4	0.7%	100.0%	2	0.5%	100.0%	2	0.6%	100.0%
2048 - 2900	Very Large	0	0.0%	100.0%	0	0.0%	100.0%	0	0.0%	100.0%	0	0.0%	100.0%
2900 - 4096	Very Large	0	0.0%	100.0%	0	0.0%	100.0%	0	0.0%	100.0%	0	0.0%	100.0%
	TOTAL	354	100.0%		601	100.0%		428	100.0%		363	100.0%	

* Divisions based on 1/2 phi scale.